Supporting information

Biobased catalyst-free Covalent Adaptable Networks based on CF_3-activated synergistic aza-Michael exchange and transesterification

Dimitri Berne[a], Baptiste Quienne[a], Sylvain Caillol[a], Eric Leclerc[a,*], Vincent Ladmiral[a,*]

[a] ICGM, Université Montpellier, CNRS, ENSCM, Montpellier, France

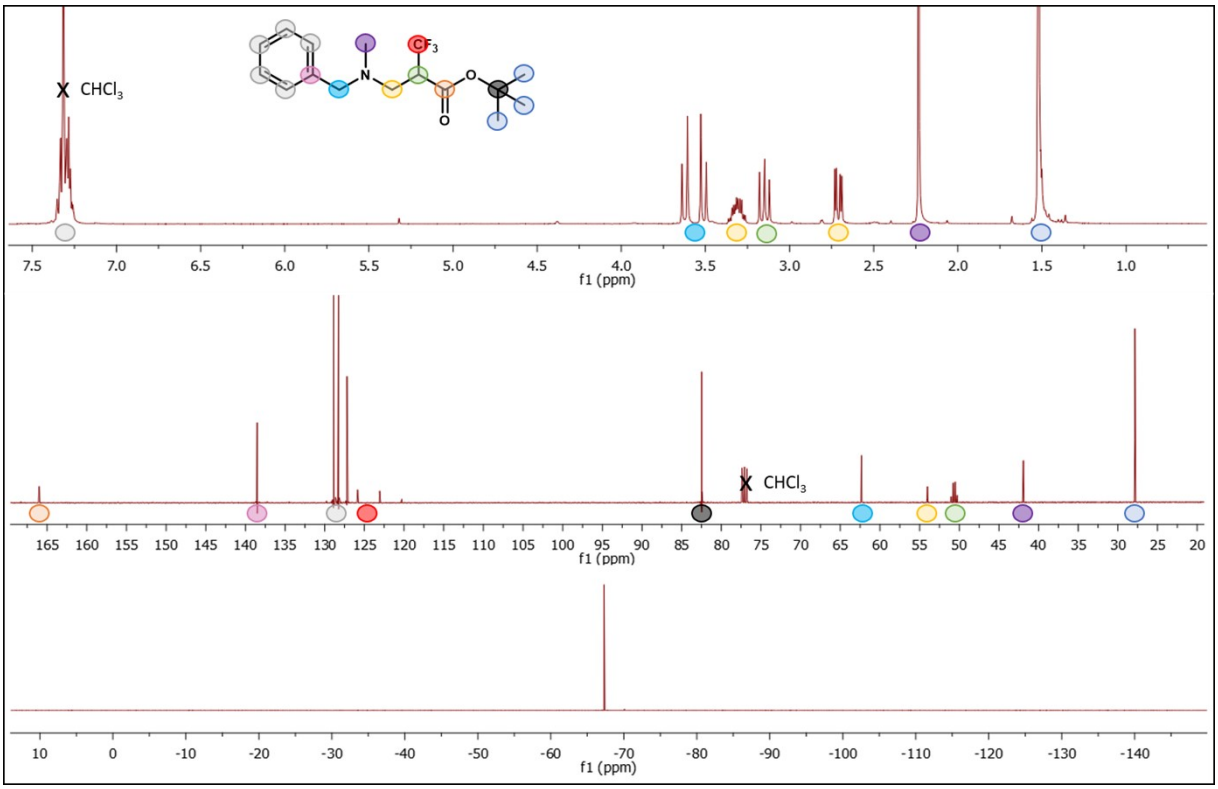

Figure S1: ^{1}H (top), ^{13}C (mid) and ^{19}F (bot) NMR spectra of BMA-MAF-TBE in $CDCl_3$ at 25 °C.

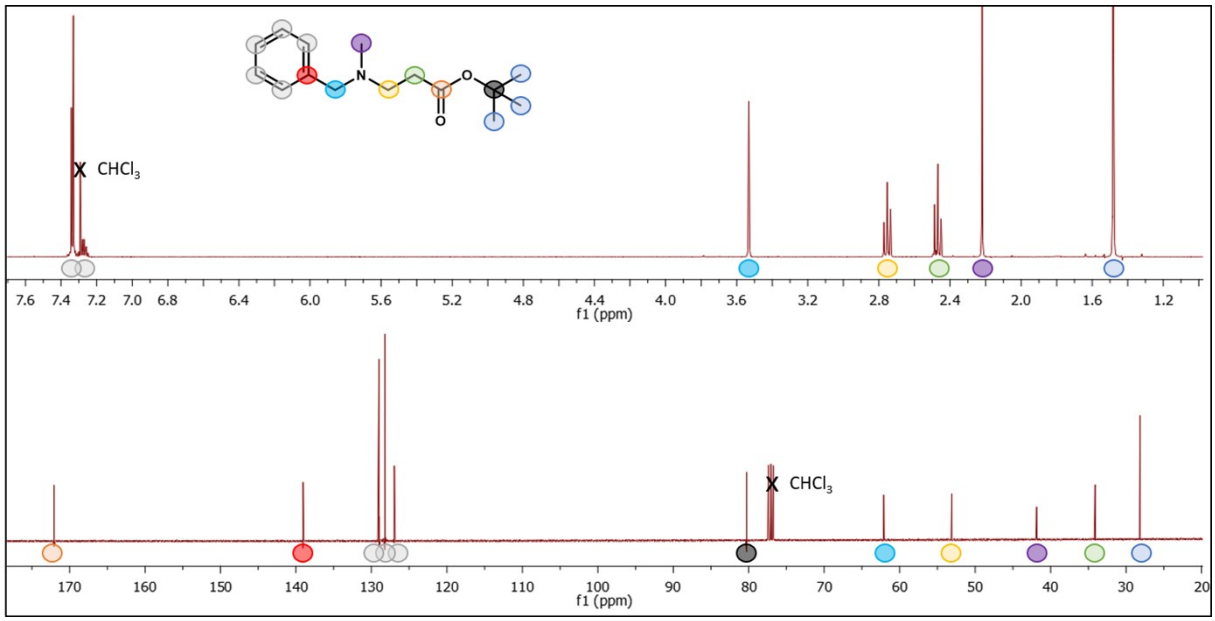

Figure S2. ^{1}H (top) and ^{13}C (bot) NMR spectra of BMA-A-TBE in $CDCl_3$ at 25 °C.

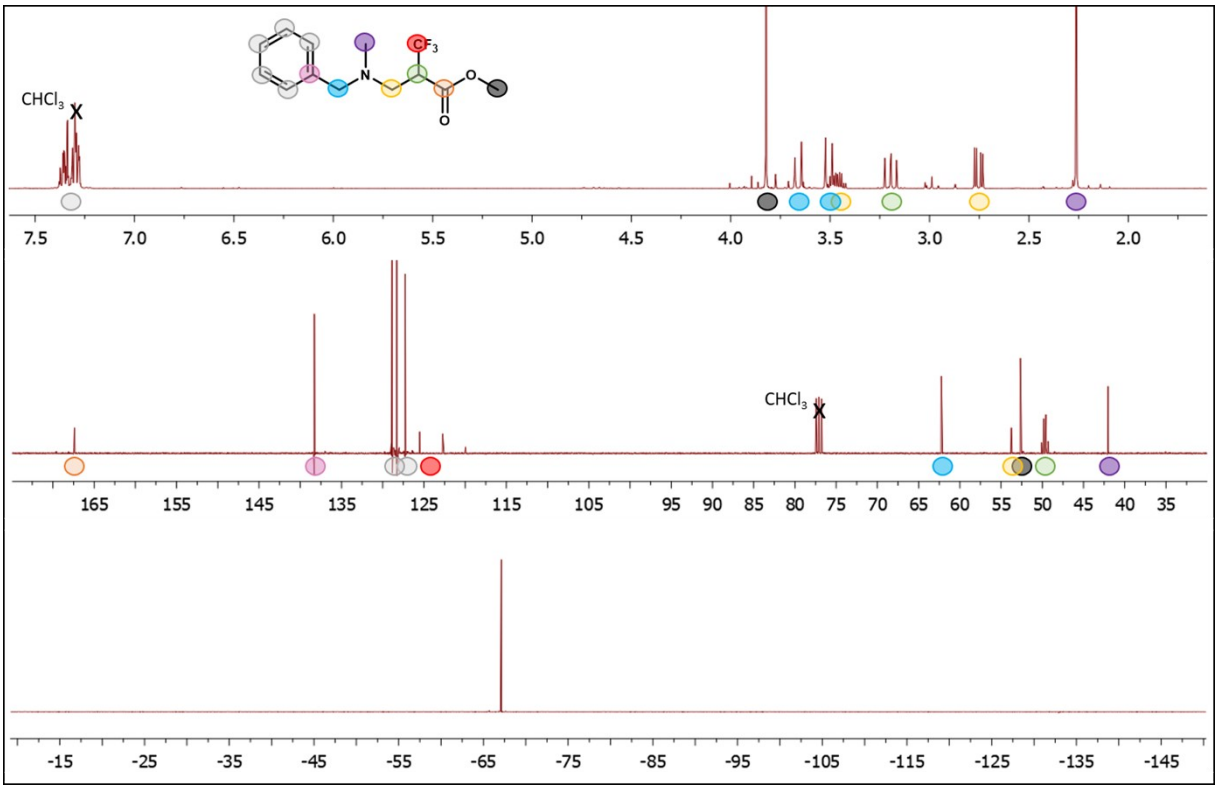

Figure S3: ^{1}H (top) and ^{13}C (bot) NMR spectra of BMA-MAF-Me in $CDCl_3$ at 25 °C.

Figure S4: ^{1}H (top) and ^{13}C (bot)) NMR spectra of BMA-A-Me in $CDCl_3$ at 25 °C.

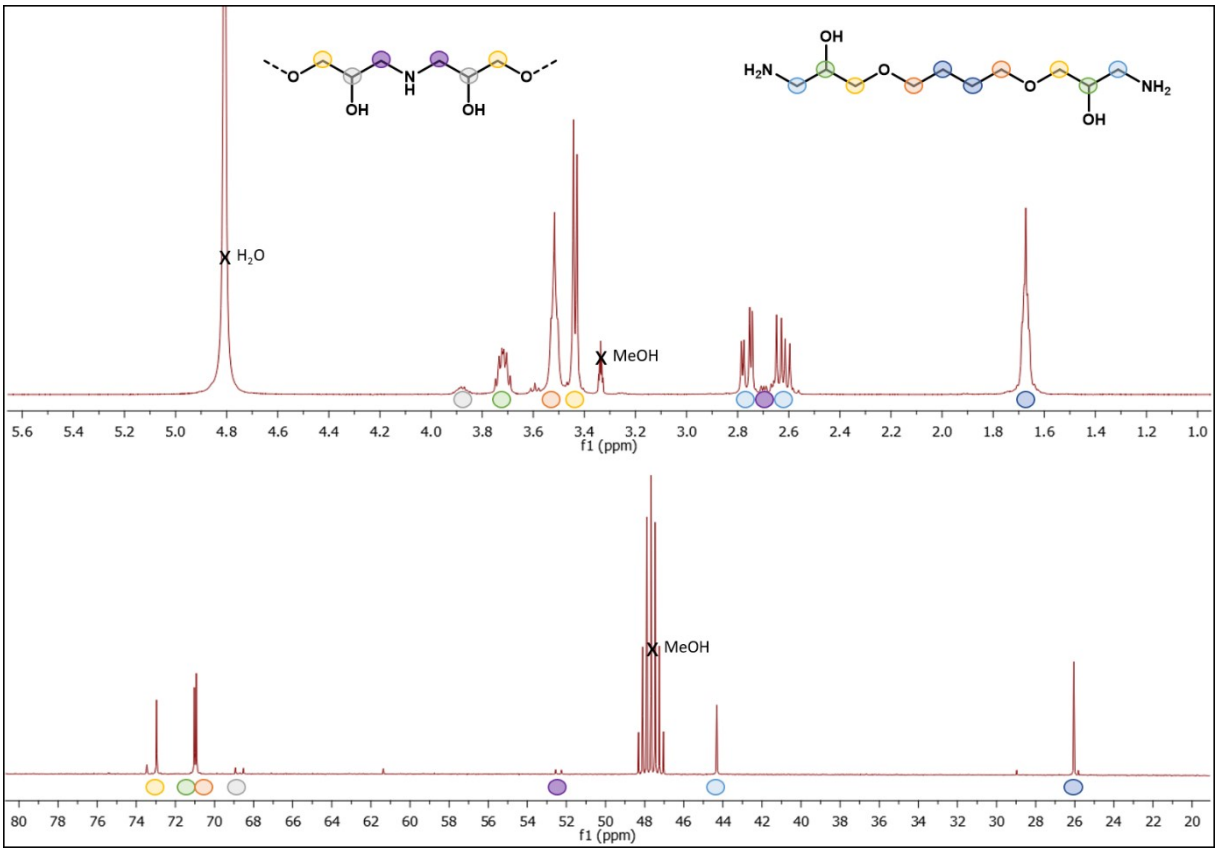

Figure S5 : ^{1}H (top) and ^{13}C (bot) NMR spectra of BD-β-HA in MeOD at 25 °C.

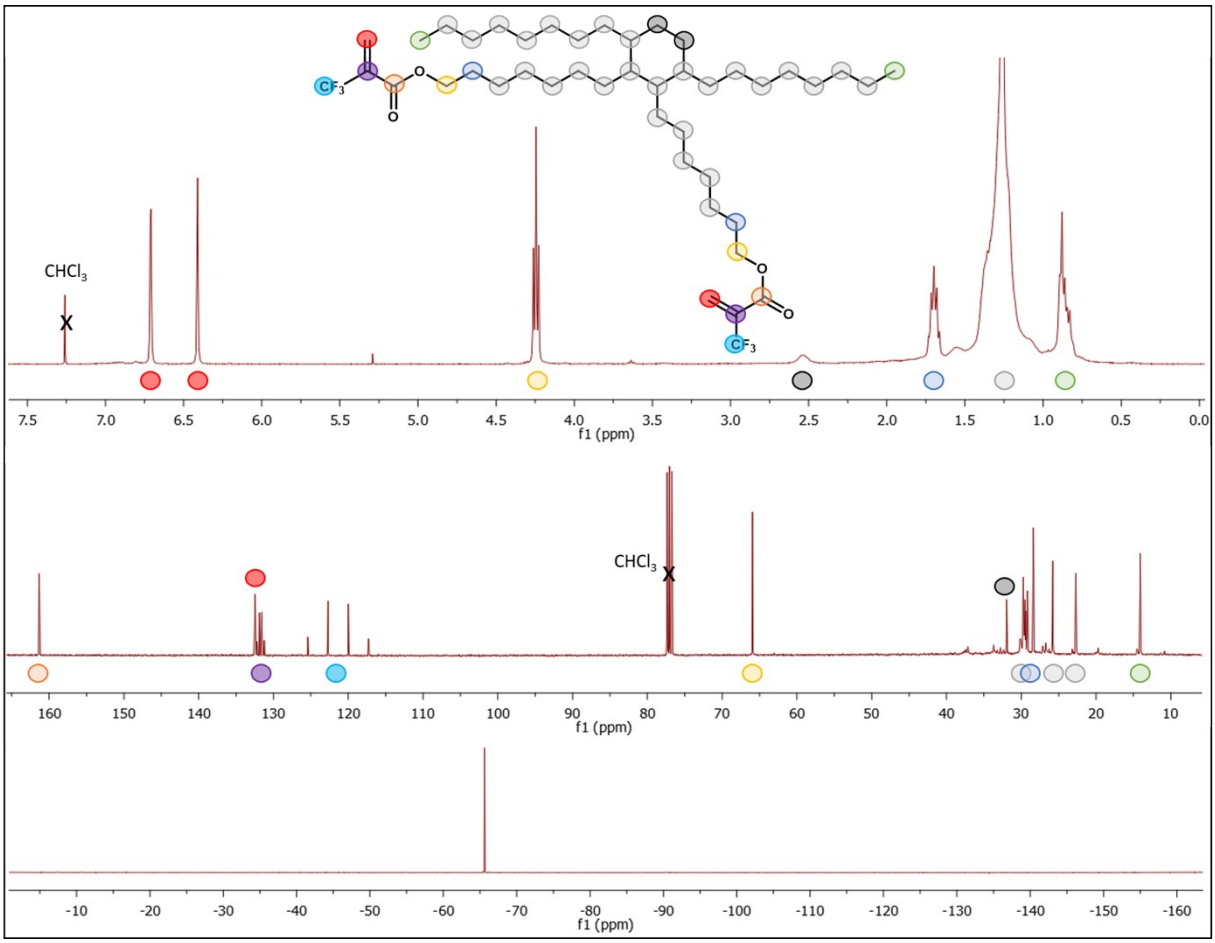

Figure S6: ^{1}H (top), ^{13}C (mid) and ^{19}F (bot) NMR spectra of Pripol-(MAF)$_2$ in $CDCl_3$ at 25 °C.

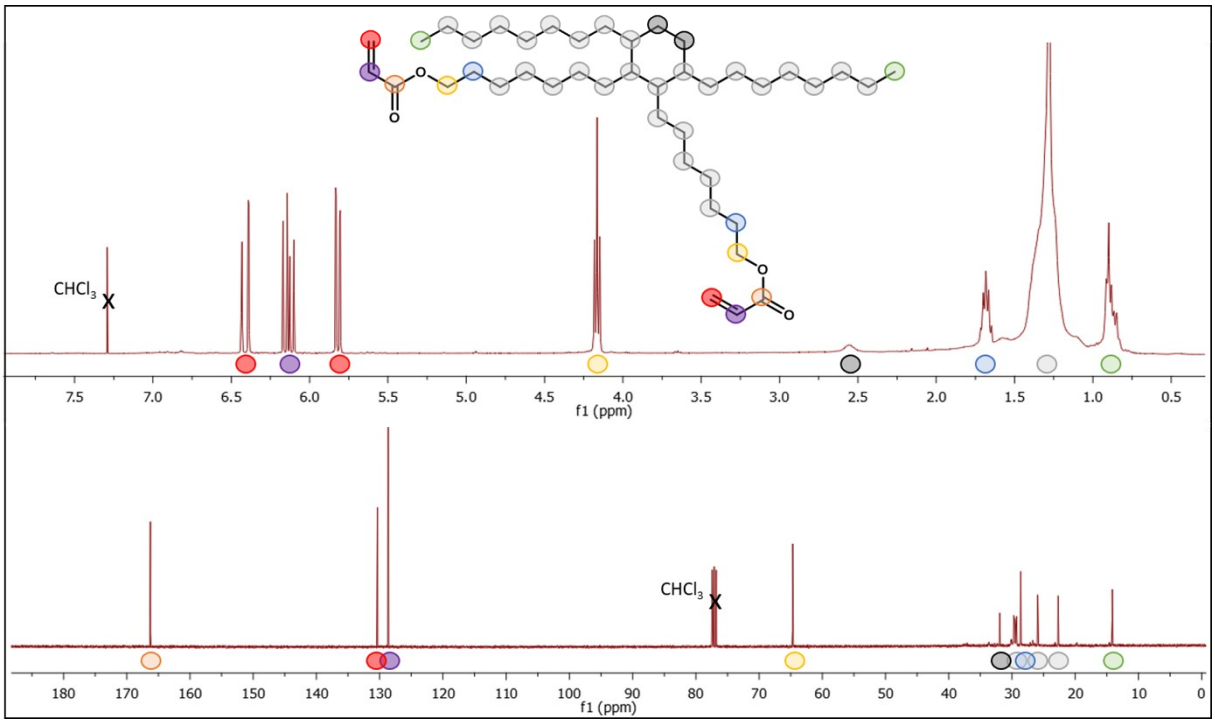

Figure S7: ^{1}H (top) and ^{13}C (bot) NMR spectra of Pripol-A$_2$ in $CDCl_3$ at 25 °C.

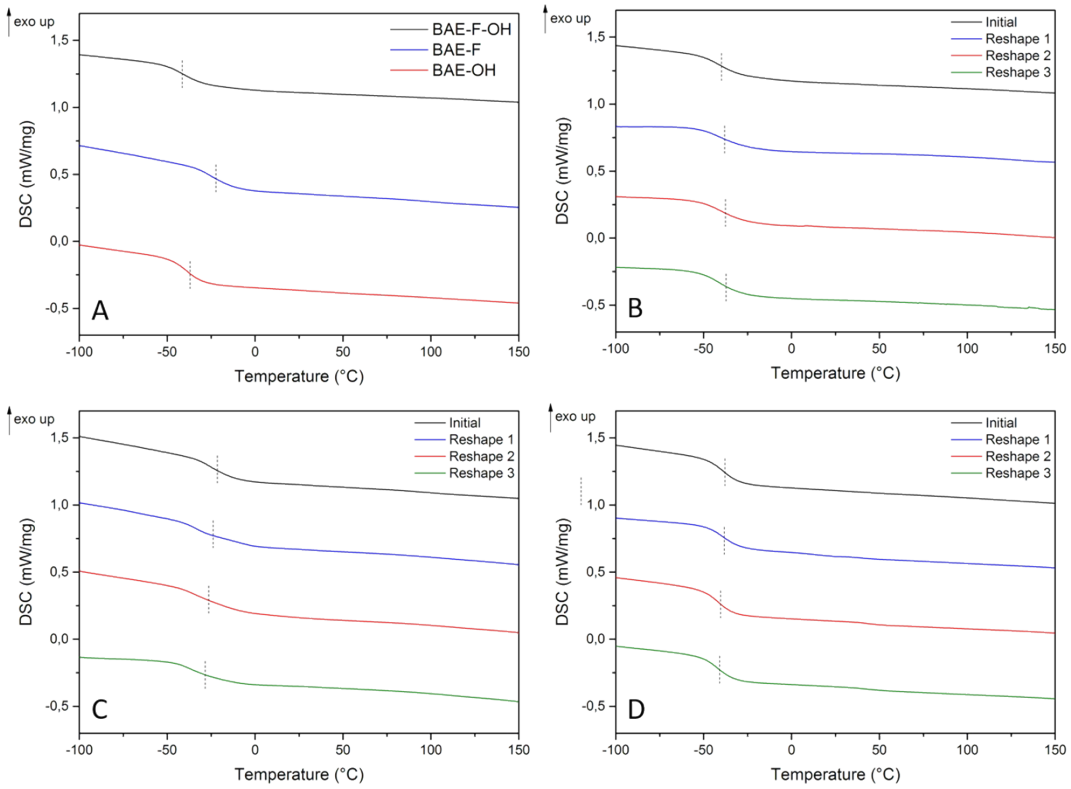

Figure S8: DSC analyses of initial BAE materials (A), BAE-F-OH (B), BAE-F (C) and BAE-OH over 3 reshaping cycles (D).

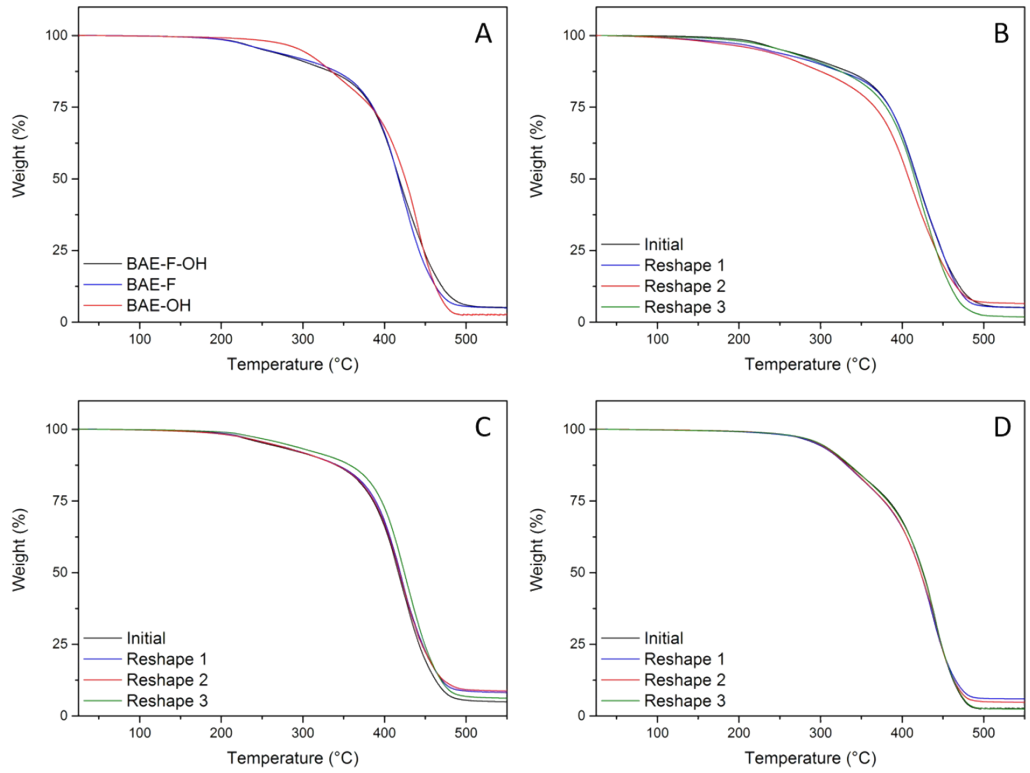

Figure S9: TGA analyses of initial BAE materials (A), BAE-F-OH (B), BAE-F (C) and BAE-OH over 3 reshaping cycles (D).

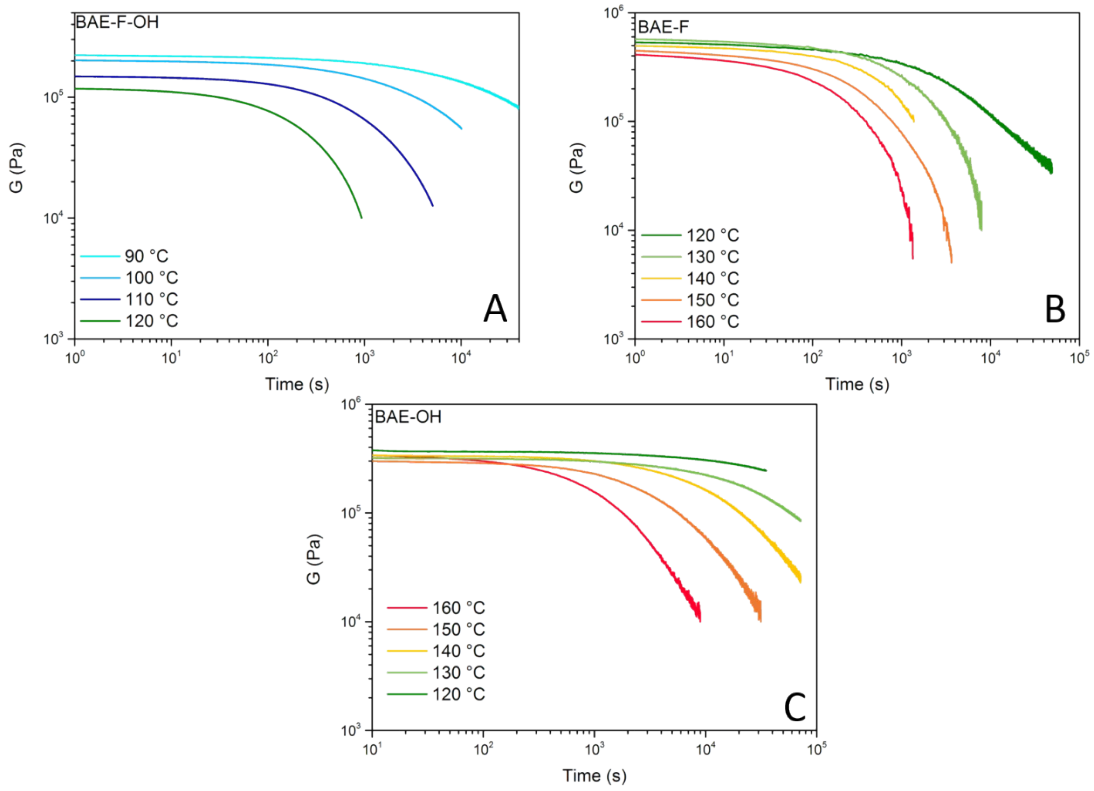

Figure S10. Non-Normalized stress-relaxation curves at different temperatures for a 1 % strain A) for BAE-F-OH, B) for BAE-F and C) for BAE-OH.

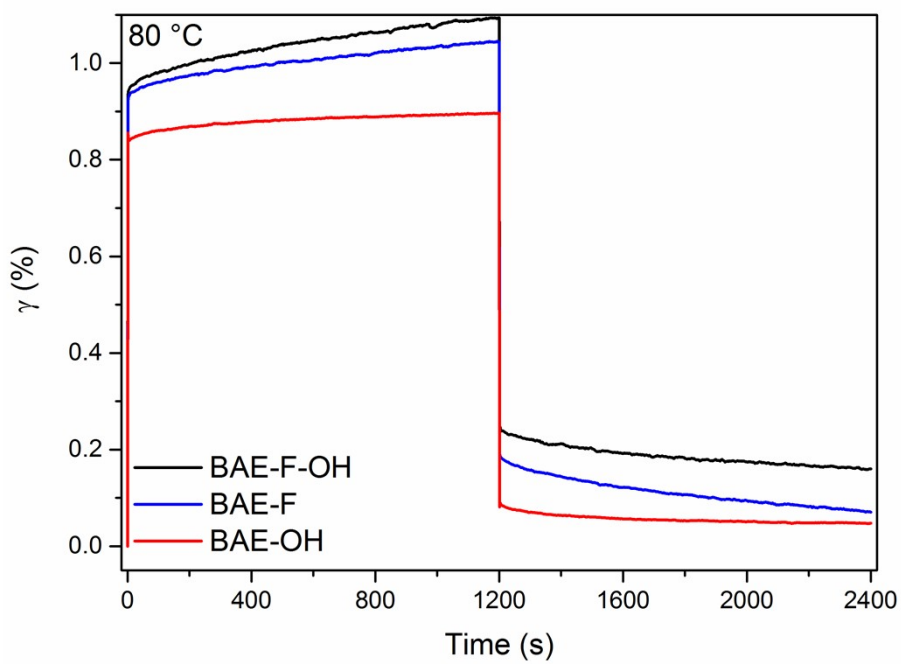

Figure S11: Creep and recovery data for BAEs at 80 °C for an applied stress of 2 kPa.

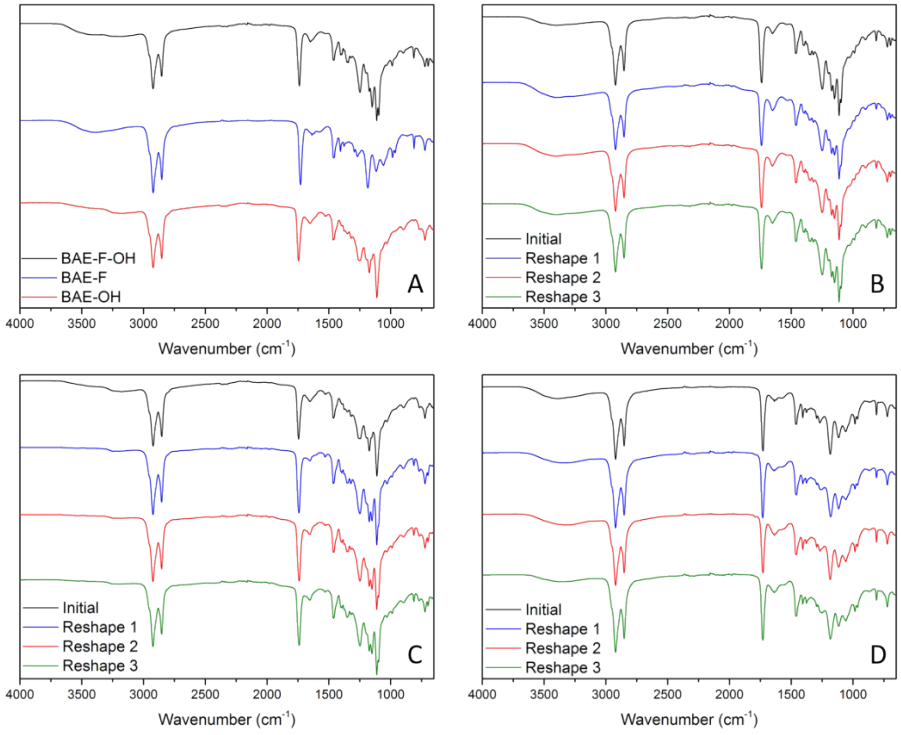

Figure S12: FTIR spectra of initial BAE materials (A), BAE-F-OH (B), BAE-F (C) and BAE-OH over 3 reshaping cycles (D).

Table S1: T_g,$T_{d5\%}$, DMA data, swelling index and gel content values of BAE materials over the reshaping cycles.

	BAE-F-OH						
	$T_{d5\%}$ (°C)	T_g (°C)	T_α (°C)	E'_{glassy} (GPa)[a]	$E'_{rubbery}$ (MPa)[b]	SI (%)	GC (%)
Initial	252	-38	-23	1.8	3.4	307	86
Reshape 1	234	-39	-30	0.9	1.5	288	83
Reshape 2	225	-39	-25	0.8	2.1	312	84
Reshape 3	252	-40	-30	2.0	2.6	315	83

	BAE-F						
	$T_{d5\%}$ (°C)	T_g (°C)	T_α (°C)	E'_{glassy} (GPa)[a]	$E'_{rubbery}$ (MPa)[b]	SI (%)	GC (%)
Initial	255	-22	-25	1.5	2.9	251	91
Reshape 1	260	-23	-25	1.5	2.3	199	89
Reshape 2	260	-26	-24	0.9	2.3	197	90
Reshape 3	277	-27	-25	1.5	2.5	202	87

	BAE-OH						
	$T_{d5\%}$ (°C)	T_g (°C)	T_α (°C)	E'_{glassy} (GPa)[a]	$E'_{rubbery}$ (MPa)[b]	SI (%)	GC (%)
Initial	297	-38	-33	1.9	2.1	288	83
Reshape 1	295	-38	-21	1.2	1.9	310	77
Reshape 2	297	-41	-28	1.3	1.8	317	72
Reshape 3	299	-41	-25	1.2	1.2	341	68

[a] Determined at T_α – 50 °C

[b] Determined at T_α + 50 °C

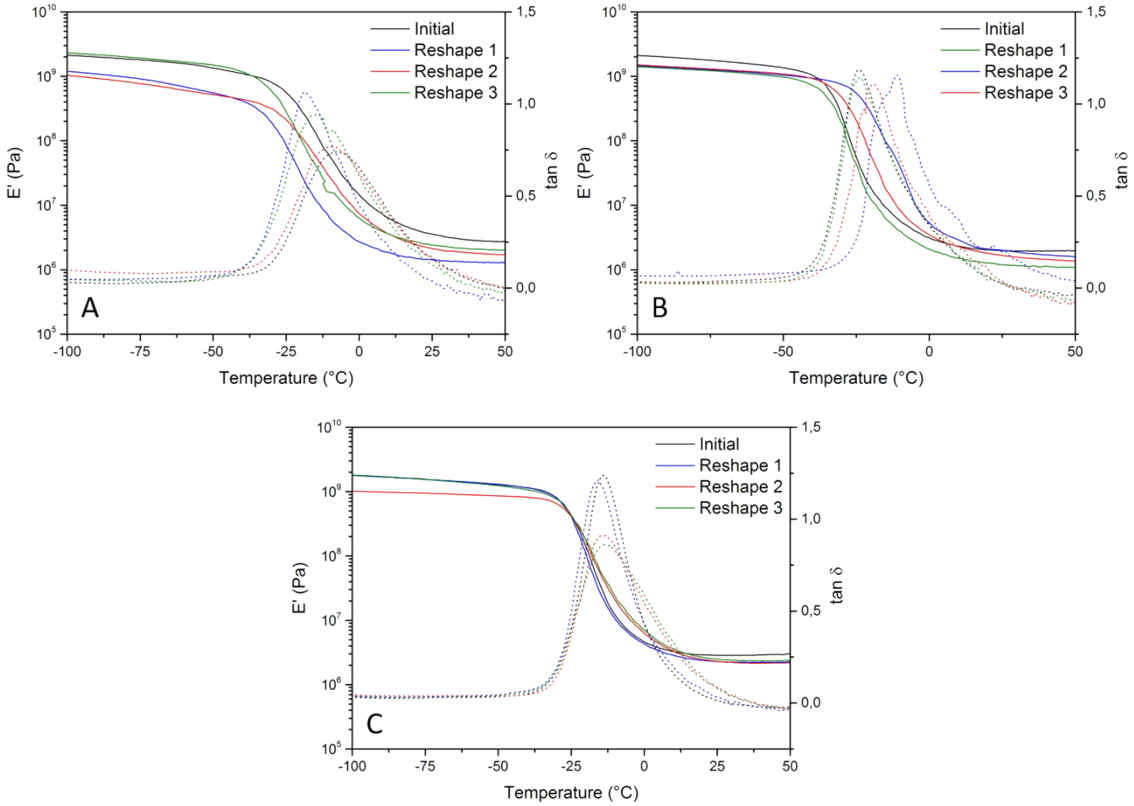

Figure S13: DMA analyses of BAE-F-OH (A), BAE-F (B) and BAE-OH (C) over three reshaping cycles.